Draft version 1.0

CEPC NOTE

CEPC_ANA_HIG_2015_XXX

April 6, 2017

Branch ratio measurement of $H \to WW^*$ at CEPC

LIAO Libo[a,b], LI Gang[b], RUAN Manqi[b], LI Kang[a], and XU Qingjun[a]

[a]Hangzhou Normal University
[b]Institute of High Energy Physics

Abstract

It's a note for $e^+e^- \to ZH, Z \to ee, H \to WW^*$ channel analysis.

- **Title:** Branch ratio measurement of $H \to WW^*$ at CEPC.
- **Author list:** it will be provided by the CEPC Collaboration, and will be made available on their website. On the front page, you should name "The CEPC Collaboration" as author.
- **Abstract:** Based on a Monte Carlo sample with planed lumonisity of $5ab^{-1}$ at CEPC, measurement of H to WW^* has been performed under full simulation. In this analysis, two decay modes of WW^*, which are $WW^* \to l^+l^-\nu\bar{\nu}$ and $WW^* \to l\nu jj$, are studied.

E-mail address: liaolb@ihep.ac.cn

Contents

1 Introduction

The precise measurements of properties of the Higgs boson become a must after its discovery [1]. Dedicated Higgs factories are therefore needed. The LHC is a perfect Higgs factory, but limited by the huge QCD background, large theoretical and systematic uncertainties, the accuracies of Higgs measurements are limited to o(5-10%) level. Therefore, it's hard to measure the propoties of Higgs boson, test the SM and research the new physics presicely.

On the other hand, an electron positron collider provides unique physics opportunity to the Higgs boson measurements. It can measure the absolute values of the Higgs boson couplings, the Higgs boson width, and is sensitive to Higgs exotic decay mode searches. The Higgs program at an e^+e^- collider is highly complementary to that of proton colliders. Therefore, multiple e^+e^- facilities has been proposed.

The CEPC is a circular e^+e^- collider with a total circumference of 50 - 100km. It is expected to deliver one million Higgs boson, almost 100% detected and reconstructed, in 10 years operation with 2 detectors. Such a sample would allow the accuracy of Higgs boson couplings to 0.1-1% level, one order of magnitude better than the HL-LHC extrapolation.

By giving nominal center-mass of energy, $\sqrt{s}$ = 250 GeV and non-polarized beam at the CEPC, the nominal Higgs bosons are produced through the Higgsstrahlung which is dominant, and Vector boson fusion processes, shown in Figure 1.

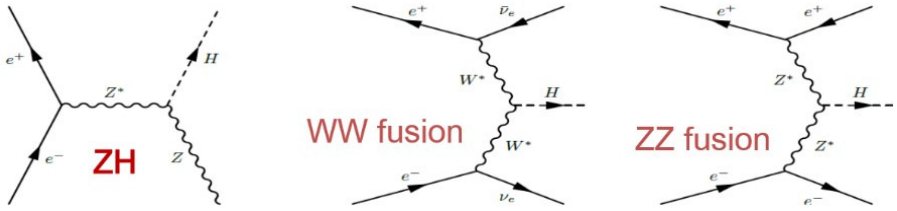

Figure 1: Feynman diagram of production of Higgs boson at CEPC

1.1 Class of signal processs

The full simulation study of Br($H \rightarrow WW^*$) measurements at the CEPC has strong physics initersts. First of all, the nominal SM Higgs boson has 22% chance to decay into a pair of W boson, therefore this measurement is the most substantial channel to study Higgs to vector boson coupling behaviors at the CEPC. Secondly, the Br($H \rightarrow WW^*$) measurement is also a key ingredient for the determination of Higgs boson width. Last but not least, the W boson decays into various physics objects(leptons, missing energy and momentum, taus and jets), therefore it provides an excellent benchmark for the detector performance studies. A series of Br($H \rightarrow WW^*$) full simulation study has been performed and status of these studies would be reported in this manuscript.

The $H \rightarrow WW^*$ events at the CEPC could be classified into 50 different channels according to final states of events. Giving one million Higgs bosons, the expected yield for $H \rightarrow WW^*$ events with different final states are presented in Table 1. Our simulation studies has covered the following channels, which is classified into 4 kinds according to the number of jets in the final states.

W boson decay \ Z boson decay	ee	$\mu\mu$	$\tau\tau$	$\nu\nu$	qq
$WW^* \to e\nu e\nu$	95	89	89	612	1791
$WW^* \to \mu\nu\mu\nu$	94	87	87	601	1758
$WW^* \to e\nu\mu\nu$	188	176	176	1212	3548
$WW^* \to e\nu\tau\nu$	201	188	187	1292	3783
$WW^* \to \mu\nu\tau\nu$	109	186	186	1280	3747
$WW^* \to \tau\nu\tau\nu$	156	99	99	683	1998
$WW^* \to e\nu qq$	1195	1117	1115	7704	22560
$WW^* \to \mu\nu qq$	1184	1106	1104	7632	22349
$WW^* \to \tau\nu qq$	1263	1180	1177	8136	23825
$WW^* \to qqqq$	3764	3518	3510	24264	71051

Table 1: Excepted signal events of $Z \to X, H \to WW^*, WW^* \to X$. The gray area means there are no jets in signal events. The green district represents the class of two jets. The four jets events are indicated by magenta. And the red one repersents six jets events.

In this note, a representative analysis of each kind is reported in detail. For type of zero jet, $e^+e^- \to ZH, Z \to \mu^+\mu^-, H \to WW^*, WW^* \to e\nu\mu\nu$ decay channel has been choosed. $e^+e^- \to ZH, Z \to e^+e^-, H \to WW^*, WW^* \to \mu\nu qq$ decay channel is a candidate for type of two jets. And for four jets events, $e^+e^- \to ZH, Z \to \nu\nu, H \to WW^*, WW^* \to qqqq$ decay channel has been choosed as the typical channel. The unique channel for six jets is complicated and would be analyzed in the future.

2 MC sample

2.1 Simulation and analysis tool

This analysis is performed with a simulated data of integrated luminosity of 5000fb^{-1}, and the cross section at $\sqrt{s} = 250$ GeV is shown in Figure 2. For all signal, which Higgs mass of $m_H = 125$ GeV is assumed, and background events are generated by Whizard 1.95 included ISR. The detector model, cepc_v1, is simulated by Gent4. Particle reconstruction is done by particle-flow algorithm, Arbor. Charged particle idendifications are done by LICH, which is a TMVA based charged particle identification using high graularity calorimeter. The ee-k_T clustering algorithm is used in jet clustering and the b-tagging probabilities is given by LCFIPlus package.

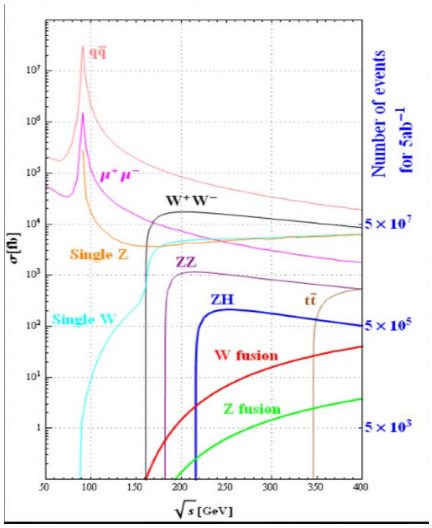

(a)

	240GeV	250GeV
qq	54662	50216
$\mu^+\mu^-$	4685	4405
single Z	4538	4734
single W	5086	5144
W^+W^-	16004	15484
ZZ	1079	1033
ZH	203	212
W fusion	5.36	6.72
Z fusion	0.50	0.63

(b)

Figure 2: 2(a): The distribution of cross sction of the Standard Model when center mass of system is near 250 GeV. 2(b): The specific value of cross section of the main Standard Model when center mass of system is 240 GeV and 250 GeV

The Standard Model background contain two femions background and four femions background. Two femions background include processes of bhabha scatter, $\mu^+\mu^-$, $\tau^+\tau^-$, $\nu\bar{\nu}$ and $q\bar{q}$. Four femions background consist of rest of the Standard Model background and Higgs Background. Higgs background is the ZH process except for the signal process.

2.2 Pre-selection

After counting the total background, the number of the Standard Model is more than 70 million. However, because of lack of computer resource, the SM background is simulated and reconstructed only a part, and many events of them have completely different event topology comparing to signal events, especially after signal catelogy according to the flavor of adjoint fermions. According to the event topology, the Higgs signals are cataloged into 4 classes, $llH(l = e, \mu)$, $\tau\tau H$, $\nu\nu H$ and qqH.

Therefore, the Standard Model background would be selected at truth level before simulation and reconstruction based on the different kinds of signal events. To make the pre-selection more consistency, reasonable and available in reconstruction level, every conditions of pre-selection should be loose at MC level, to preserve the signal almostly.

2.2.1 Pre-selection of $e^+e^- \to ZH, Z \to l^+l^-(l = e, \mu), H \to X$ decay

Compared to the Standard Model background, the most remarkable feature in $Z \to l^+l^-(l = e, \mu), H \to X$ decay channel is the combination of invariant mass and recoil mass of Z boson. Just like the real situation in detector, the best candidate of Z boson by consisted of leptons should be found. As shown in Table 2, here are two conditions of filter. Fisrt one is invariant mass of l^+l^-. The second is corresponding recoil mass.

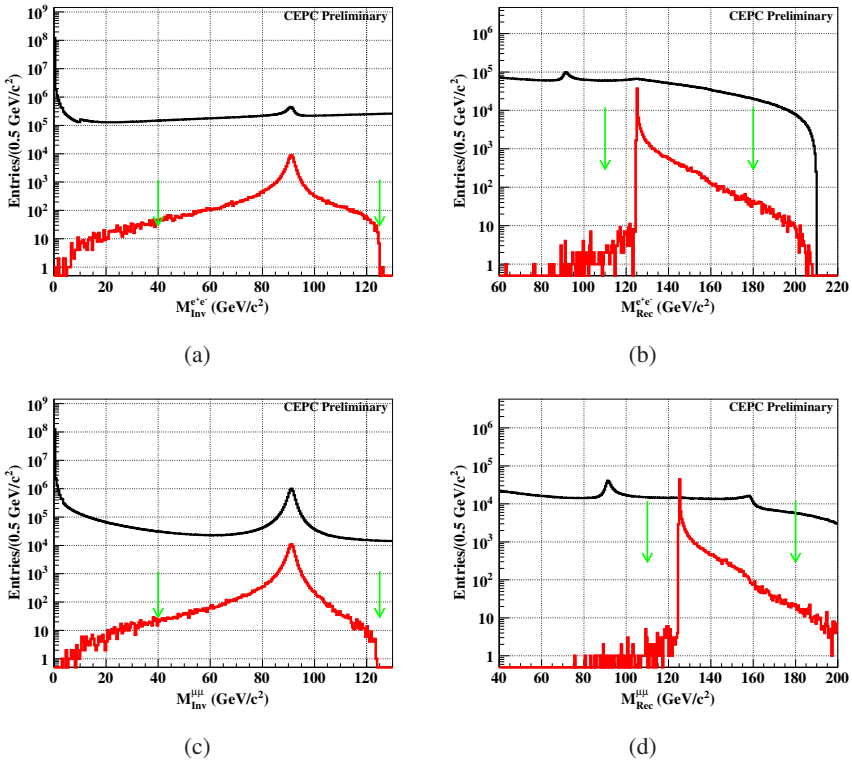

Figure 3: The distribution of invariant mass and recoil mass of the best candidate of Z boson. Red line is the distribution of Higgs signal. Black line is the distribution of the Standard Model background. TOP: These two plots are the mass distribution of $Z \to e^+e^-, H \to X$ decay. Bottom: The left is invariant mass distribution and right is recoil mass distribution of $Z \to \mu^+\mu^-, H \to X$ decay

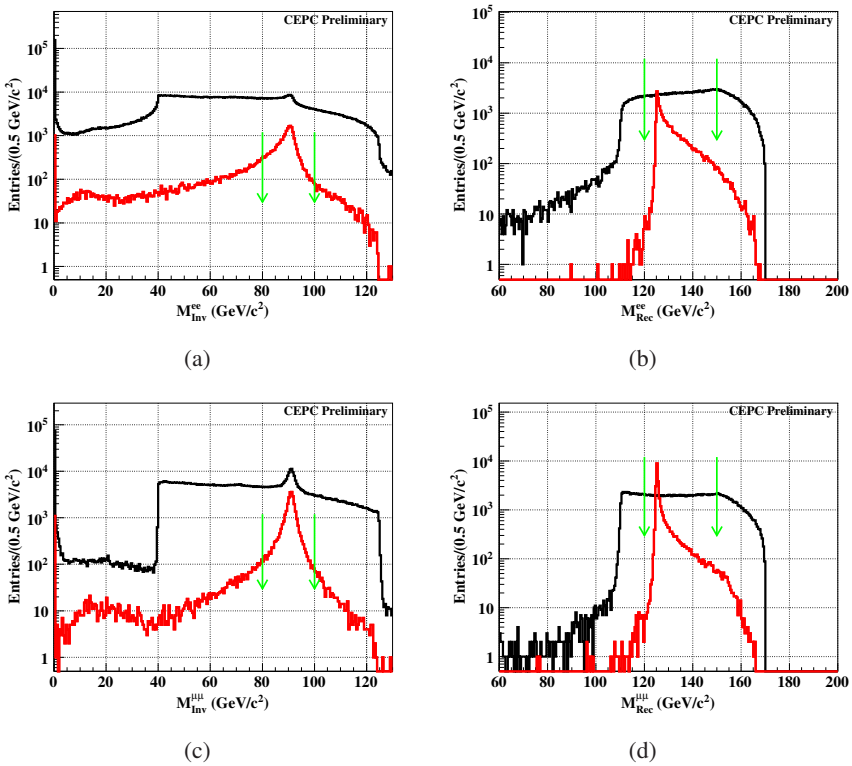

Figure 4: The distribution of invariant mass and recoil mass of the best candidate of Z boson in full simulation. Red line is the distribution of Higgs signal. Black line is the distribution of the Standard Model background. TOP: These two plots are the mass distribution of $Z \to e^+e^-, H \to X$ decay. Bottom: The left is invariant mass distribution and right is recoil mass distribution of $Z \to \mu^+\mu^-, H \to X$ decay

Process of signal	eeH process	$\mu\mu H$ process
conditions of pre-selection	$40\ \mathrm{GeV}/c^2 < M^{ee}_{Inv} < 130\ \mathrm{GeV}/c^2$ $110\ \mathrm{GeV}/c^2 < M^{ee}_{Rec} < 180\ \mathrm{GeV}/c^2$	$40\ \mathrm{GeV}/c^2 < M^{\mu\mu}_{Inv} < 130\ \mathrm{GeV}/c^2$ $110\ \mathrm{GeV}/c^2 < M^{\mu\mu}_{Rec} < 180\ \mathrm{GeV}/c^2$
conditions of validation	$80\ \mathrm{GeV}/c^2 < M^{ee}_{Inv} < 100\ \mathrm{GeV}/c^2$ $120\ \mathrm{GeV}/c^2 < M^{ee}_{Rec} < 150\ \mathrm{GeV}/c^2$	$80\ \mathrm{GeV}/c^2 < M^{\mu\mu}_{Inv} < 100\ \mathrm{GeV}/c^2$ $120\ \mathrm{GeV}/c^2 < M^{\mu\mu}_{Rec} < 150\ \mathrm{GeV}/c^2$

Table 2: Conditions of pre-selection in MC and validation in full simulation. Considered the resolution of detector, the conditions of validation should be more strict.

After pre-selection, signal events have been preserved more than 95% and background events have been rejected more than 99% in truth. And there are no bias after pre-selection.

2.2.2 Pre-selection of $e^+e^- \to ZH, Z \to \nu\bar{\nu}, H \to X$ decay.

Compared to eeH and $\mu\mu H$ processes. conditions of pre-selection of $\nu\nu H$ process are more difficult to choose. Because the Z boson in ZH process is decay to neutrino which is invisible in detector, it's hard to utilize the missing mass of system to distinguish signal and background clearly. For rejecting background extremely, we chose these three conditions: missing mass, total mass and total transvers momentum. In addtion, if $|cos\theta|$ of particle is larger than 0.99, it would be regard as missing particle.

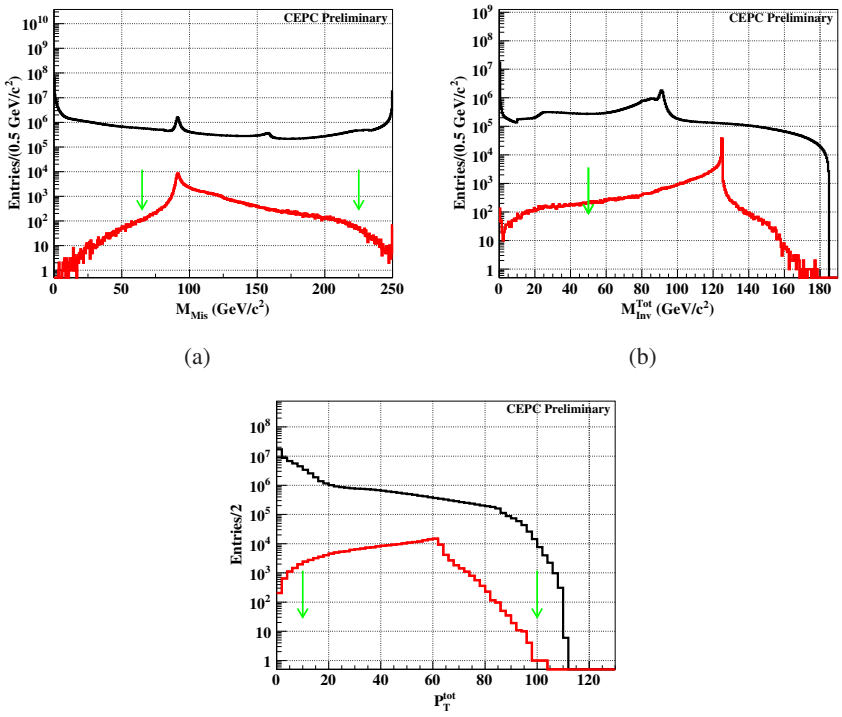

Figure 5: The distribution of missing mass, total mass and total transverse momentum in MC truth. Red line is the distribution of Higgs signal. Black line is the distribution of the Standard Model background. Top: The left is missing mass of system. The right is total mass of system. Bottom: It is the distribution of total transverse momentum of system, and the peak of background is caused by angle constraint of two femion background.

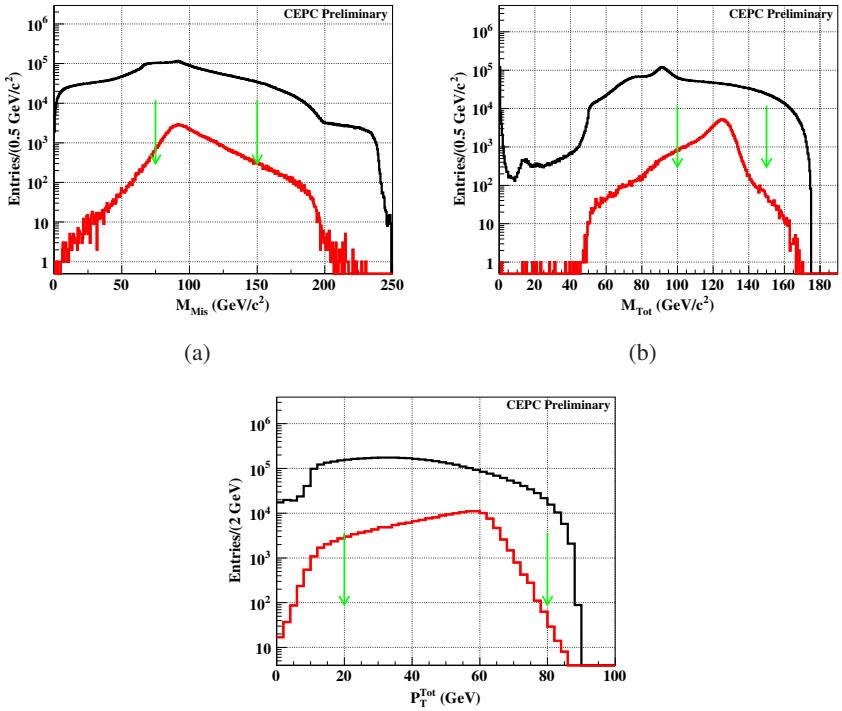

Figure 6: The distribution of missing mass, total mass and total transverse momentum in full simulation. Red line is the distribution of Higgs signal. Black line is the distribution of the Standard Model background. Top: The left is missing mass of system. The right is total mass of system. Bottom: It is the distribution of total transverse momentum of system.

Process of signal	$\nu\nu H$
conditions of pre-selection	$65\ \mathrm{GeV}/c^2 < M_{Mis} < 225\ \mathrm{GeV}/c^2$ $M_{Tot} > 50\ \mathrm{GeV}/c^2$ $10\ \mathrm{GeV}/c < p_T < 100\ \mathrm{GeV}/c$
conditions of validation	$75\ \mathrm{GeV}/c^2 < M_{Mis} < 150\ \mathrm{GeV}/c^2$ $100\ \mathrm{GeV}/c^2 < M_{Tot} < 150\ \mathrm{GeV}/c^2$ $20\ \mathrm{GeV}/c < p_T < 80\ \mathrm{GeV}/c$

Table 3: Conditions of pre-selection in MC and validation in full simulation of $\nu\nu H$ procecss

As shown in Figure 5, the distributions of signal and background are similar, so we should be careful to do filter to reject bias, and we choose the conditions as shown in Table 3. Percent of each channel has changed after pre-selection, but it makes sense for analysis.

After reconstructed, we can get distribution of the same variables, as shown in Figure 6. Considering the resolution of detector in full simulation, the conditions of validation should be more strict.

3 Measurement of $Br(H \to WW^*)$

After pre-selection, the fundamental for measurement of branch ratio is complete. Just as the mentioned before, here are too many subchannels to be described in detail, so sone typical subchannels should be represented below.

3.1 Analysis of $e^+e^- \to ZH, Z \to \mu^+\mu^-, H \to WW^*, WW^* \to e\nu\mu\nu$ decay

3.1.1 Event selection

It is a chosen channel because only two visible particles in final states from W bosons. Therefore, the background would be supressed effectively by different lepton flavors. And only leptonic decay of b-jets, W boson and τ would be survived.

Refered to the Moxin's article **??**, only few number of $ZZ \to \mu^+\mu^-\tau^+\tau^-$ decay and $ZZ \to 4\tau$ decay would not be rejected by requiring three muons and one electron and number of remain particles are less than 3. So the Higgs background would be main background compared to the Standard Model background.

Furthermore, the spatial resolution of vertex detector(VTX) of CEPC constructed with high resolution pixel sensors near the interacted point(IP) is better than 3 μm, so leptonic decay of τ and b-jet would be rejected effectively by a constructed function, which is $\sqrt{(\frac{D_0}{sigD_0})^2 + (\frac{Z_0}{sigZ_0})^2} < 5$.

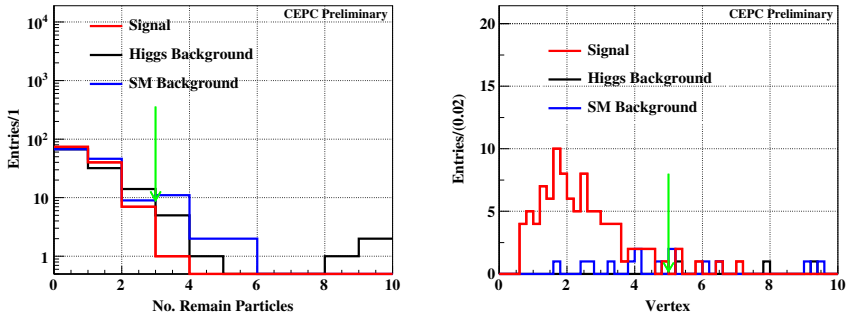

(a) (b)

Figure 7: 7(a) The No. remain particles of $e^+e^- \to ZH, Z \to \mu^+\mu^-, H \to WW^*, WW^* \to e\nu\mu\nu$ decay. Except for four tracks, there are few photons, so we can veto semi-leptonic decay and hadronic decay of background. 7(b) The distribution of Vertex of $e^+e^- \to ZH, Z \to \mu^+\mu^-, H \to WW^*, WW^* \to e\nu\mu\nu$ decay. And there are two leptons totally from W boson, so we plus the value of each lepton. And leptons from τ and b-jet would fly a long distance, so they would be rejected effectively.

After event selection in, final number of events of signal and background are in Table 4. And the main background of this channel is $e^+e^- \to ZZ \to \tau^+\tau^-\mu^+\mu^-$, as shown in Table 5.

Category	Signal	ZH background	SM background
Total	172	34624	700311
Validation of pre-selection	136	29263	117395
$N_{ZPole} = 2; N_{Isolep} = 2; l_1 = e, l_2 = \mu$	122	145	150
$N_{Remain} < 3$	121	113	122
10 GeV $< M_{Inv}^{e\mu} <$ 65 GeV	116	101	87
$M_{Missing} < 65$ GeV$/c^2$	110	26	36
$\sqrt{(\frac{D0}{sigD0})^2 + (\frac{Z0}{sigZ0})^2} < 5$	93	3	10

Table 4: The final event selection of $e^+e^- \to ZH, Z \to \mu^+\mu^-, H \to WW^*, WW^* \to e\nu\mu\nu$ decay.

Decay Chain	Final States	Number of Events
$e^+e^- \to ZZ, ZZ \to \tau^+\tau^-\mu^+\mu^-$	$\mu^+, \mu^-, \tau^+, \tau^-$	10

Table 5: Summery of total background with the same final states of signal event

3.1.2 Statistical result

After selection, we can get the distribution of recoil mass of $\mu^+\mu^-$, as shown in Figure 3.1.2.

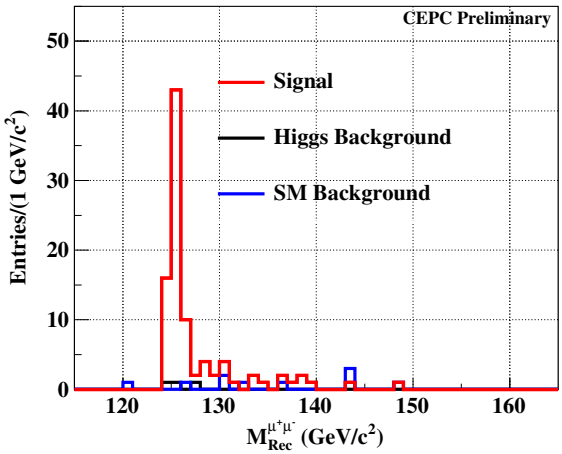

Figure 8: The distribution of recoil mass of $\mu^+\mu^-$ after event selection

Number of signal events could be got by counting,

$$N_{sig} = 93 \pm 10;$$

and N_{sig} is events of signal, the effeciency of selection $\varepsilon = 54.1\%$. Statistical uncertainty is

$$Accu. = \frac{\sqrt{S+B}}{S} = 11\%.$$

3.2 Analysis of $e^+e^- \to ZH, Z \to e^+e^-, H \to WW^*, WW^* \to \mu\nu q\bar{q}$ decay

3.2.1 Event selection

In this subchannel, number of signal events is much more lager than full-leptonic decay subchannel although it's not as clear as $e\nu\mu\nu$ channel, so we could get a higher accuracy. The final states in this subchannel are three leptons, several jets and neutrinoes which are perfomanced as missing mass. Full-leptonic decay background of τ events would be rejected by number of remain particle less than 30 and larger than 7.

As mentioned before, invariant mass and corresponding recoil mass of two leptons from initial Z boson are effective criteria to supress the Standard Model background. So validation of pre-selection, 80 GeV/c^2 < $M_{Inv}^{e^+e^-}$ < 100 GeV/c^2 and 120 GeV/c^2 < $M_{Rec}^{e^+e^-}$ < 150 GeV/c^2 are applied.

The jets come from diffenert ways,such as Higgs decay, W boson decay, Z boson decay and τ decay. Based on this, the invariant mass of jets, 10 GeV/c^2 < M_{Rec}^{di-Jet} < 95 GeV/c^2, could distinguish the signal and background well. And b-jet would not come from W boson, so we could use b-tagging to vote the b-jet background.

In signal, here is only one isolated muon from W boson and its start point is near the IP, so background of muon from τ or jet could be rejected powerfully by a function. The form of this function is similar with before, $\sqrt{(\frac{D_0}{sigD_0})^2 + (\frac{Z_0}{sigZ_0})^2} < 4$. In order to veto background of t channel, transverse momentum $p_T > 5$ GeV has applied.

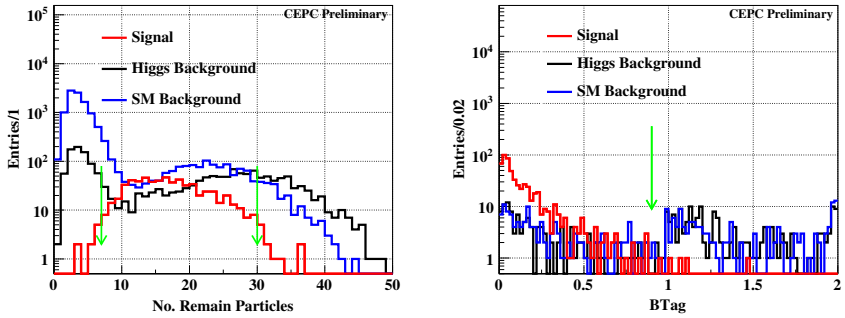

(a)

(b)

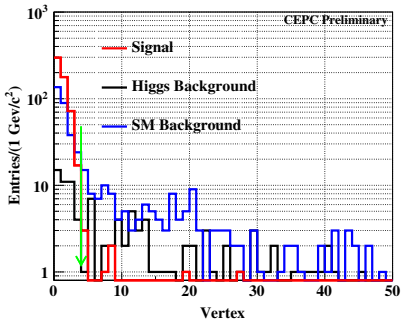

(c)

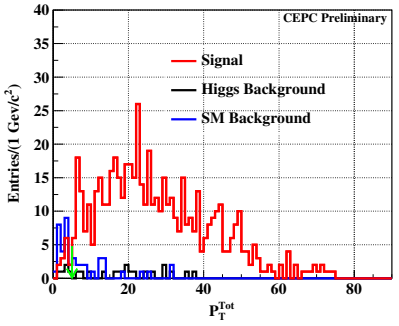

(d)

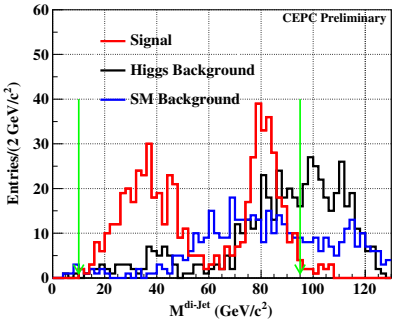

(e)

Figure 9: 9(a) The No. remain particles of $e^+e^- \to ZH, Z \to e^+e^-, H \to WW^*, WW^* \to \mu\nu q\bar{q}$ decay. Because it is semi-leptonic decay channel, so the No. remain particles should between it of hadronic decay and full-leptonic decay. 9(b) The distribution of Btag, we plus the Btag value of each jets because of existing two jets. And because no b-jet decay from W boson, the value of them should be less than 1. 9(c) The distribution of vertex of lepton. Leptons from τ and b-jet would fly a long distance, so they would be rejected effectively. 9(d) The distribution of transverse momentum p_T. Transverse momentum of t channel would be lower than of s channl. 9(e) The distribution of di-jet invariant mass, the high-side could distinguish the jets from Z boson or H boson.

After the selection as shown in Table 6, the background are supressed almostly. Table 7 shows the main background after event selection.

Category	Signal	ZH background	SM background
Total	1149	36319	1303847
$N_{ZPole} = 2; N_{Isolep} = 1; N_{Jets} = 2; l = \mu$	1022	1970	21857
Validation of pre-selection	631	1207	2987
$7 < N_{Remain} < 30$	603	540	436
$15\ \mathrm{GeV}/c^2 < M_{Rec}^{di-Jet} < 95\ \mathrm{GeV}/c^2$	589	284	278
$Btag < 0.9$	584	116	131
$M_{Missing} < 45\ \mathrm{GeV}/c^2$	571	72	102
$\sqrt{(\frac{D0}{sigD0})^2 + (\frac{Z0}{sigZ0})^2} < 4$	564	23	45
$p_T > 5$ GeV	551	18	21

Table 6: The final event selection of $e^+e^- \to ZH, Z \to e^+e^-, H \to WW^*, WW^* \to \mu\nu q\bar{q}$ decay

Decay Chain	Final States	Number of Events
$e^+e^- \to ZH, Z \to e^+e^-, H \to WW^* \to \tau\nu q\bar{q}$	$e^+, e^-, \tau, \nu, 2q$	14
$e^+e^- \to e^+e^-Z, Z \to qq$	$e^+, e^-, 2q$	13

Table 7: Summery of total background with the same final states of signal event

3.2.2 Statistical result

After selection, the distribution of recoil mass of e^+e^- is shown in Figure 3.3.2.

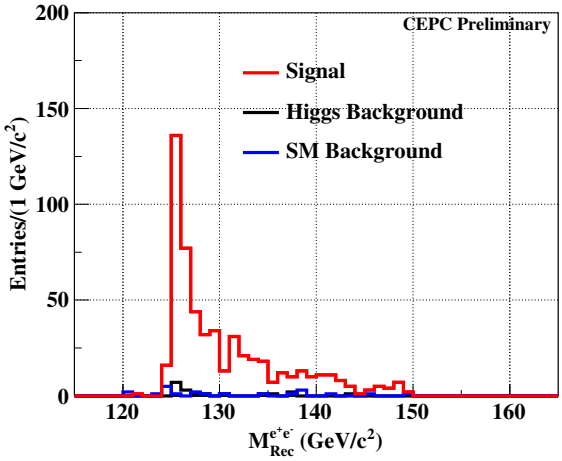

Figure 10: The distribution of recoil mass of $\mu^+\mu^-$ after event selection

We can get the number of signal events by counting,

$$N_{sig} = 551 \pm 24;$$

and N_{sig} is events of signal, the effeciency of selection $\varepsilon = 48.0\%$. Statistical uncertainty is

$$Accu. = \frac{\sqrt{S+B}}{S} = 4.5\%.$$

3.3 Analysis of $e^+e^- \to ZH, Z \to \nu\bar{\nu}, H \to WW^*, WW^* \to q\bar{q}q\bar{q}$ decay

3.3.1 Event selection

This is a hadronic decay channel and no isolated lepton. Lost of the Standard Model background would not be supressed by no isolated lepton and at least two jets. The number of final particles is required to be larger, $No._{Particles}^{Total} > 20$, because the final particles are producted a lot after hadronization of quarks. And fraction of hadronic process would be enhanced a lot by this requirement.

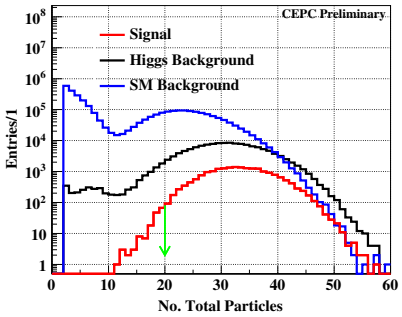

Figure 11: The number of total final particles distribution. To count the total number, the enengy threshold of each particle is required, $E > 1$ GeV

The the jet clustering has been done twice. At the first time, two jets are clustered to reject the two jets background, such as $H \to q\bar{q}$ decay of Higgs background, ZZ semi-leptonic decay and "single $Z - nu$" semi-leptonic decay process of the Standard Model background. These two jets are required $Btagging < 0.9$, $Cos\theta_{2jets} > 0.87$ and $\Sigma|M_{Inv}^{2jet}| > 50\ \mathrm{GeV}/c^2$. And at the second time, four jets are required. In this situation, the characterizes of signal are more important. Y value is effective to distinguish the signal and background. The event is required to have $Y_{34} > 0.005$. According to these four jets, we would get two components which are the combination of four momentum of among two jets. The invariant mass of one of the components should be near the mass peak of the W boson, and the jets in the other part are regard as from virtual W boson decay. Figure 13(b) shows the distribution of these two component. The combined functions are:

- $65\ \mathrm{GeV}/c^2 < M_{Inv}^{Real4jet} < 85\ \mathrm{GeV}/c^2$;
- $15\ \mathrm{GeV}/c^2 < M_{Inv}^{Virt4jet} < 50\ \mathrm{GeV}/c^2$;
- $M_{Inv}^{Virt4jet} > -7/3 M_{Inv}^{Real4jet} + \frac{605}{3}\ \mathrm{GeV}/c^2$;

$M_{Inv}^{Real4jet}$ means invariant mass of two jets which are regard as jets decay from real W boson. And $M_{Inv}^{Virt4jet}$ means invariant mass of two jets which are regard as jets decay from virtual W boson.

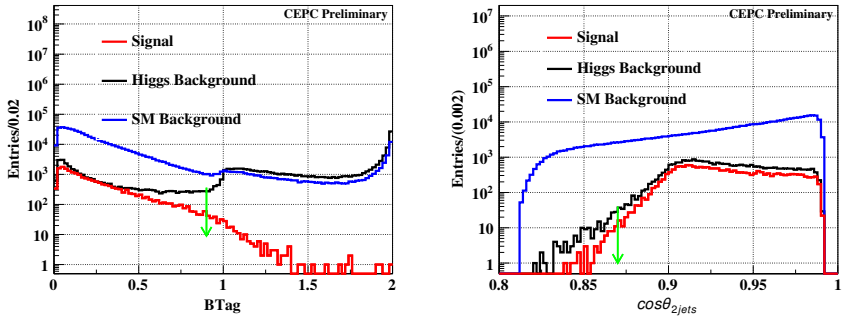

(a)

(b)

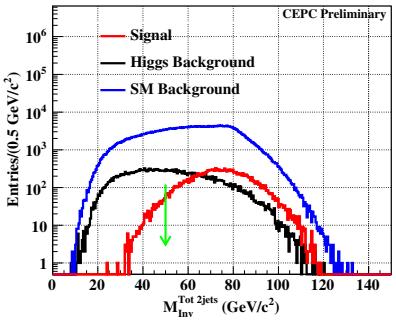

(c)

Figure 12: 12(a) B-tag of two jets distribution. We plus the value of B-tag of each jet, 12(b) The distribution of angle between two jets. The boost of Higgs is larger, so the angle between two jets in signal should be smaller its in background. 12(c) The distribution of total invariant mass of two jets. The number of jets in almost background is two. The invariant mass of each jet should be smaller.

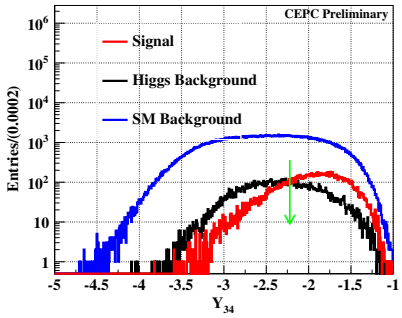

(a)

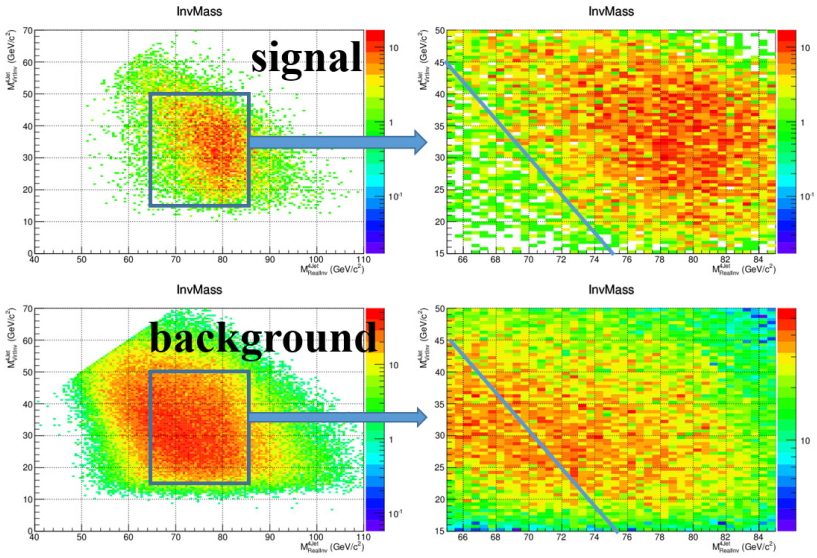

(b)

Figure 13: 13(a) Y value distribution. 13(b) 2D scatter diagram of invariant mass of real and virtual W boson. The left plot representes the distribution of signal, and the right is of background. In order to distinguish the signal and background effectively, a hexagonal mass window is applied.

177 After the event selection, the signal is protected near 50% as shown in Table 8

Category	Signal	ZH background	SM background
Total	23938	208200	21314314
Validation of pre-selection	20405	143765	3166923
$N^{Tot}_{Particle} > 20$	19681	124112	537839
$Btag < 0.9$	19349	28857	477099
$Cos\theta_{2jets} > 0.87$	19298	28673	433563
$\Sigma\lvert M^{2jet}_{Inv}\rvert > 50$ GeV	18621	14793	309919
$Y_{34} > 0.005$	15183	6919	122866
Combined Variable	9022	3075	38226

Table 8: The final event selection of $e^+e^- \to ZH, Z \to \nu\bar{\nu}, H \to WW^*, WW^* \to q\bar{q}q\bar{q}$ decay

Decay Chain	Final States	Number of Events
$e^+e^- \to ZH, Z \to \nu\bar{\nu}, H \to c\bar{c}$	$\nu, \bar{\nu}, c, \bar{c}$	192
$e^+e^- \to ZH, Z \to \nu\bar{\nu}, H \to b\bar{b}$	$\nu, \bar{\nu}, b, \bar{b}$	352
$e^+e^- \to ZH, Z \to \nu\bar{\nu}, H \to gg$	$\nu, \bar{\nu}, 2g$	2028
$e^+e^- \to ZH, Z \to \nu\bar{\nu}, H \to ZZ^*, ZZ^* \to q\bar{q}q\bar{q}$	$\nu, \bar{\nu}, 2q, 2\bar{q}$	439
$e^+e^- \to ZZ, ZZ \to \nu\bar{\nu}q\bar{q}$	$\nu, \bar{\nu}, q, \bar{q}$	3115
$e^+e^- \to ZZ, ZZ \to \tau^+\tau^- q\bar{q}$	$\tau^+, \tau^-, q, \bar{q}$	910
$e^+e^- \to WW, WW \to \tau\nu q\bar{q}$	$\tau, \nu, q, \bar{q}$	30398
$e^+e^- \to WW, WW \to \mu\nu q\bar{q}$	$\mu, \nu, q, \bar{q}$	277
$e^+e^- \to \nu\bar{\nu}Z, Z \to q\bar{q}$	$\nu, \bar{\nu}, q, \bar{q}$	1838
$e^+e^- \to e\nu W, W \to e\nu q\bar{q}$	$e, \nu, q, \bar{q}$	1398
$e^+e^- \to qq$	$2q$	262

Table 9: Summery of main background with the same final states of signal event

3.3.2 Statistical result

After selection, we can get the distribution of missing mass, as shown in Figure **??**.

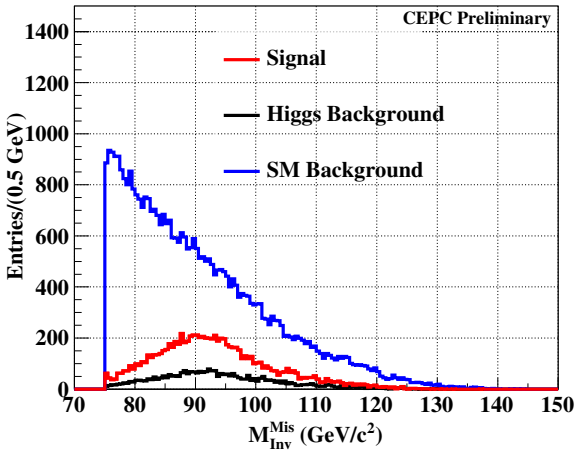

Figure 14: The distribution of recoil mass of $\mu^+\mu^-$ after event selection

We can get the number of signal events by counting,

$$N_{sig} = 9022 \pm 224;$$

and N_{sig} is events of signal, the effeciency of selection $\varepsilon = 37.7\%$. Statistical uncertainty is

$$Accu. = \frac{\sqrt{S+B}}{S} = 2.5\%.$$

4 Results

The function of measurement of branch ratio of $H \to WW^*$ is

$$Br(H \to WW^*) = \frac{N_{sig}}{N_{total} \cdot Br_{rel.} \cdot \varepsilon}$$

$N_{total} = \mathcal{L} \times \sigma_{ZH}$ means total number of events of ZH process; $Br_{rel.}$ means relative branch ratio for $Br(H \to WW^*)$ measurement, including branch fraction of Z boson and W boson; ε means the efficiency of event selection of signal; N_{sig} means the events of signal after event selection.

Category	Signal	Relative uncertainty	Efficiency of selection
$Z \to e^+e^-; H \to WW^* \to evev$	20±7	35%	25.0%
$Z \to e^+e^-; H \to WW^* \to \mu\nu\mu\nu$	44±8	18.2%	43.1%
$Z \to e^+e^-; H \to WW^* \to ev\mu\nu$	53±8	15.1%	27.6%
$Z \to e^+e^-; H \to WW^* \to evqq$	435±23	5.3%	37.0%
$Z \to e^+e^-; H \to WW^* \to \mu\nu qq$	551±24	4.5%	48.0%
$Z \to \mu^+\mu^-; H \to WW^* \to evev$	23±5	21.7%	25.8%
$Z \to \mu^+\mu^-; H \to WW^* \to \mu\nu\mu\nu$	39±7	18%	44.8%
$Z \to \mu^+\mu^-; H \to WW^* \to ev\mu\nu$	93±10	11%	54.1%
$Z \to \mu^+\mu^-; H \to WW^* \to evqq$	573±25	4.0%	51.7%
$Z \to \mu^+\mu^-; H \to WW^* \to \mu\nu qq$	756±30	4.4%	68.4%
$Z \to \nu\bar{\nu}; H \to WW^* \to qqqq$	9022±224	2.5%	37.7%

Table 10: Statistic uncertainty of Signal and Relative uncertainty

	Total events N	$Br(W \to l\nu)$	$W \to qq$	$Z \to l^+l^-$	$Z \to qq$
Mean value	1060000	10.86%	67.41%	3.3658%	69.91%
Uncertainty	±4000	±0.09%	±0.27%	±0.0023%	±0.06%

Table 11: Relative data for measurement of branch ratio

After analysis, the relative uncertainty of signal of 11 subchannels is given in Table 10, and the result of each branch ratio is given by other collabration in Table 11. The relative uncertainties of $Z \to X$, $W \to X$ and N_{Total} are negligible. Relative statistical uncertainty $\Delta Br(H \to WW^*)/Br(H \to WW^*)$ is 1.62%.

5 Summary and conclusion

11 subchannel of $H \to WW^*$ process have been analyzed at CEPC. The integrated luminosity of 5000fb$^-$1 and the mass of Higgs boson of 125 GeV are assumed. The obtained result of accuracy for branch ratio is 1.62%.

Recently, only about 15% data has been analyzed. With the CEPC R&D goes by, the result of analysis would be optimized continuously. In the future, $Z \to qq, H \to WW^* \to qqqq$ channel would be analyszed, which would improve the accuracy effectively for measurement of branch ratio. Furthermore, CEPC is also a Z boson factory, and it would give us a great support. On the one hand, the precision of measurement result about Z boson would be improved, and it would be helpful for precise measurement at CEPC. On the other hand, a huge sample would be producted at Z pole, and it would help us to study the performance of detector better and reduce the systematic uncertainty.

Later on, there are three parts to be considered. At first, systematic uncertainty has not be discussed. And we would do it in the future. Secondly, the isolated lepton finder algorithm is not a general algorithm, and needs to be optimized and improved, but it is suitable for recent research. At last, events of signal

are got by counting, and we should learn the distribution of signal and background deeper and do a fit to improve precision of analysis.

6 Acknowledgements

Thanks Dr. LI Gang and Dr. RUAN Manqi greatly for their guidance and their constructive arguements. And thanks my colleagues, Mr. CHEN Zhenxing and Mr. WEI Yuqian who build a good basement for me, Dr. MA Bingsong and Dr. MO Xin who are engaged in generator, simulation and reconstruction of samples, Dr. WANG Feng who help me solve some technical problems.

References

[1] R. M. CHEN Zhenxing, LIU Shuai,, "Measurement of higgs to ww at cepc." Available from the cepc note web page: Http://cepcdoc.ihep.ac.cn/docdb/0000/000041/001/ww_v1.0.pdf.

Appendices

A Isolated leptons' condition

Isolated leptons tagging is a key in WW^* analysis, espcially in jets environment, so a good iaolated leptons algorithm could decide our analysis accuracy. We will introduce the isolated leptons algorithm below:
There are two key conditions. The first one is lepton identification that a good PFA could help us. The second is isolated conditions, cone angle of lepton and the ratio of energy in cone angle and lepton's energy, shown in Table 12.

E_{lepton}	Leptons' flavor	Full-leptonic Decay		Semi-leptonic Decay	
		Cone Angle[rad]	E_{Cone}/E_{Lepton}	Cone Angle[rad]	E_{Cone}/E_{Lepton}
5 GeV – 10 GeV	Muon	0.15	0.25	0.15	0.7
	Electron	0.3	1.1	0.3	0.9
10 GeV – 15 GeV	Muon	0.15	0.35	0.15	0.25
	Electron	0.3	0.75	0.3	0.75
> 15 GeV	Muon	0.15	0.3	0.15	0.25
	Electron	0.25	0.55	0.25	0.6

Table 12: Isolated lepton condition